

Reach-Through Avalanche Photodiodes in Soft X-ray Detection

Andrea L. Gouvea, *Student Member, IEEE*, Aldo Antognini, Franz Kottmann, Randolph Pohl, and Luis M. P. Fernandes

Abstract—Reach-through avalanche photodiodes (RT-APDs) from Hamamatsu Photonics, with different active areas, 5×5 and 3×5 mm², were investigated to evaluate their suitability for the muonic helium Lamb shift experiment. The gain has been determined as a function of voltage and temperature for both prototypes. As expected, it increases with increasing bias voltage and with decreasing temperature. The gain variation with temperature is smaller than -2% per °C even for higher bias voltages applied to the RT-APD. The non-linearity between gain obtained for X-rays and visible light pulses has been investigated for different temperatures. The non-linearity was found to increase with decreasing temperature. For example at 350 V, it is as high as 25% at -20 °C and about 10% at 20 °C. The RT-APDs performance for the detection of 8 keV X-rays has been investigated. The best energy resolution was achieved for the larger prototype for a temperature of 0 °C. The minimum energy resolution values, between 9.2 and 9.9%, were obtained for gains between 55 and 80. The minimum detectable energy observed is about 0.2 keV for the higher gain region, for both RT-APDs, investigated, with no significant improvement at lower temperatures.

Index Terms—Energy resolution, gain non-linearity, minimum detectable energy, reach-through avalanche photodiodes (RT-APDs), soft X-ray detection.

I. INTRODUCTION

AVALANCHE PHOTODIODES (APDs) are monolithic devices made of silicon, where photons are converted into free charge carriers in the active volume with further multiplication in the p-n junction, giving rise to an avalanche process via impact ionization [1]. Nowadays, they are extensively used in various fields such as high-energy physics, medical imaging, aerospace applications, optical communications, gamma-rays

detection as photosensors coupled to scintillators, soft X-rays detection, among others [2], [3], [4], [5], [6], [7], [8], [9], [10], [11]. The main advantages of APDs are low bias voltage, compactness, robustness, broad spectral response and insensitivity to magnetic field. Their high gain and consequently higher signal-to-noise ratio make them more attractive than Si PIN diodes. They present however some drawbacks when compared to photomultiplier tubes (PMTs), such as lower gains, gain dependence on temperature and voltage fluctuations, large excess noise factor and small active areas [1], [11], [12]. Moreover, their enhanced quantum efficiency and insensitivity to magnetic fields [11] make them interesting for specific experiments when comparing with PMTs.

Reach-through avalanche photodiodes (RT-APD) are silicon APDs with a thicker depletion region, which makes them more efficient for X-rays detection below 20 keV [13], [14] than regular APDs. The main disadvantage remains the manufacturing technique of large area prototypes, which is not sustainable and reliable. Companies such as Hamamatsu Photonics and Perkin Elmer are producing RT-APDs, although with small detection areas [15], [16].

The main objective of this work is to investigate the performance of RT-APDs from Hamamatsu Photonics with different active areas, 3×5 and 5×5 mm², for low-energy X-rays detection in view of the muonic helium Lamb shift experiment [17], where 8 keV X-rays need to be detected with good efficiency. In the predecessor experiment, muonic hydrogen Lamb shift, [18], [19], large area avalanche photodiodes from Radiation Monitoring Devices (RMD) [20] were used to detect 2 keV X-rays. Those detectors were first selected for their high detection efficiency, which is above 90% for 2 keV X-rays. In addition, they present other interesting properties like good energy resolution, of about 15%, compactness, fast time response, large active areas of 13.5×13.5 mm² and finally insensitivity to magnetic fields up to (5 T) [11], [18], [19]. However, for 8 keV X-rays, the RMD LAAPDs have an efficiency of only 40%, motivating the investigation of RT-APDs as an alternative.

The performance characteristics of two RT-APD prototypes, with active areas of 3×5 and 5×5 mm², have been measured. Gain, minimum detectable energy and energy resolution have been determined as a function of bias voltage and temperature. The gain non-linearity between X-rays and visible light was also evaluated.

II. EXPERIMENTAL SETUP

Fig. 1 shows a picture of the two RT-APDs prototypes from Hamamatsu Photonics used in the present study. They present a

Manuscript received November 19, 2013; revised May 23, 2014; accepted June 06, 2014. Date of publication July 25, 2014; date of current version August 14, 2014. This work was supported in part by FEDER through the Programa Operacional Factores de Competitividade (COMPETE) and in part by National funds through the Fundação para a Ciência e Tecnologia (FCT) in the frame of the project PTDC/FIS/102110/2008. A. L. Gouvea was supported by Grant SFRH/BD/66731/2009 from FCT. R. Pohl was supported by ERC starting Grant 279765.

A. L. Gouvea and L. M. P. Fernandes are with the Instrumentation Center, University of Coimbra, P-3004-516 Coimbra, Portugal (e-mail: andrea.gouvea@gian.fis.uc.pt; pancho@gian.fis.uc.pt).

A. Antognini and F. Kottmann are with the Institute for Particle Physics, ETHZ, CH-8093 Zürich, Switzerland (e-mail: aldo@phys.ethz.ch; franz.kottmann@psi.ch).

R. Pohl is with the Max-Planck-Institut für Quantenoptik, 85748, Garching, Germany (e-mail: randolf.pohl@mpq.mpg.de).

Color versions of one or more of the figures in this paper are available online at <http://ieeexplore.ieee.org>.

Digital Object Identifier 10.1109/TNS.2014.2331461

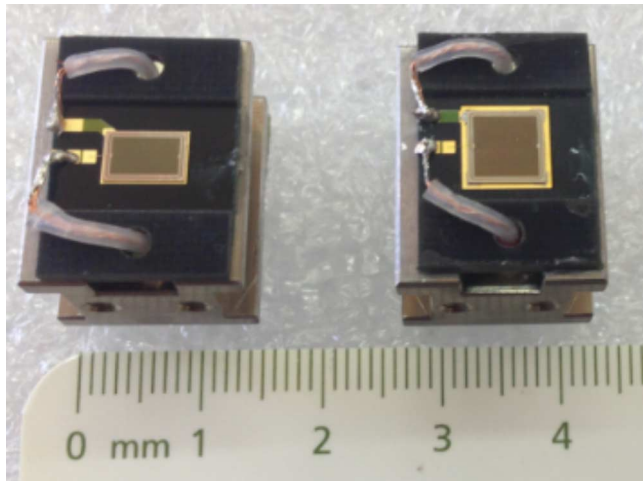


Fig. 1. Reach-through avalanche photodiodes from Hamamatsu Photonics with different active areas, 3×5 and 5×5 mm². The APDs are mounted on Ti pieces for efficient cooling.

TABLE I
OPERATIONAL PARAMETERS OF THE RT-APDS PROVIDED BY
HAMAMATSU PHOTONICS AT 26 °C

Size	Active Area (mm ²)	Breakdown Voltage (V)	Gain (at V=200V)
5×5	25	623	39
3×5	15	510	57

depletion region of 130 μ m. One is rectangular with 3×5 mm² active area and the other one is square with 5×5 mm² active area. The RT-APDs were glued to PCB and mounted on a titanium piece for efficient cooling, and connected to RAL 108A low-noise charge-sensitive preamplifiers [21]. A typical signal at the RAL preamplifiers output has about 200 ns rise-time, more than 100 μ s fall-time and amplitudes of about 100-200 mV. According to the datasheets provided by the manufacturer, the relevant parameters of each type of RT-APD are listed in Table I.

The RT-APDs, together with the respective preamplifiers, were placed inside a vacuum chamber for temperature control. Cooling of the system is provided by an alcohol system connected to the preamplifier mounting. Temperature stabilization within ± 0.1 °C is obtained. The preamplifier was connected to an Ortec research amplifier with integration and differentiation time constants of 0.5 μ s, followed by a multi-channel analyzer (AmpTek Pocket MCA 8000A). A positive high voltage power supply was used to polarize the RT-APDs. A LED emitting in the visible light region, operating in pulse mode with -10 V amplitude and 100-500 ns width, was used. The LED was coupled to a light guide to transport the light pulses towards the APD surface. A ⁶⁵Zn radioactive source emitting 8.0 keV K_{α} and 8.9 keV K_{β} X-rays was placed at 10.3 mm distance from the detector surface, together with the light guide. No collimator was used, the full active area of the detectors was irradiated by the two radiation sources.

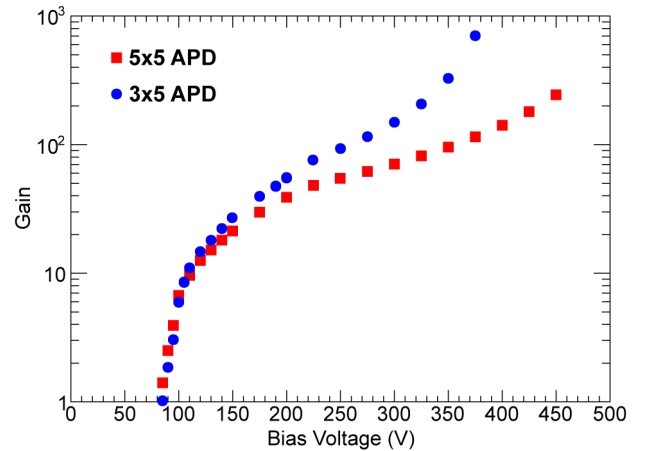


Fig. 2. Absolute gain for both 3×5 and 5×5 mm² prototypes as a function of bias voltage at 0 °C, obtained for visible light LED pulses.

III. GAIN MEASUREMENTS

The APD strong gain dependence on the applied bias voltage is well known, as well as the gain variation with temperature. Another relevant aspect is the gain non-linearity between X-rays and visible light due to space charge effects in X-ray detection, leading to local gain variations [2], [4], [12], [22], [23]. The gain curves provided by the manufacturer at room temperature (25 °C) were used as a reference for our measurements. The normalization was made for a bias voltage of 200 V, which corresponds to a gain of 39 for the 5×5 prototype and 57 for the 3×5 prototype (Table I).

A. Gain Determination

The unitary gain was not determined in our measurements as no signals were detected at low voltages (for both X-rays or light pulses). The absolute gain was determined at 0 °C for both RT-APDs as a function of bias voltage, using LED pulses, as shown in Fig. 2. The gain was obtained by normalizing the light pulse amplitude to the manufacturer gain (Table I). A correction factor was introduced by comparing the relative amplitudes obtained in each RT-APD at 25 °C and 0 °C. For lower bias voltages, the gain drops abruptly. This effect is probably due to the recombination of the primary electrons under very low electric fields, leading to partial charge collection. As seen in Fig. 2, the gain is higher for the 3×5 prototype at higher voltages, while it is about the same for both RT-APDs for lower voltages.

B. Gain Non-Linearity

The gain non-linearity takes place at higher gains due to high signal current densities produced by X-rays. The gain obtained for X-rays is lower than the one obtained for visible light and the difference increases with bias voltage. The non-linearity owes essentially to space charge effects with a consequent reduction of the local electric field, as well as local heating, due to the point-like nature of the X-rays interaction. To evaluate the gain non-linearity, the ratio between pulse amplitudes for 8 keV X-rays and visible light pulses from the LED, simultaneously illuminating the RT-APD active area, was determined, as described in [12]. Fig. 3 presents the gain obtained for X-rays and visible light as a function of bias voltage at 25 °C, for the

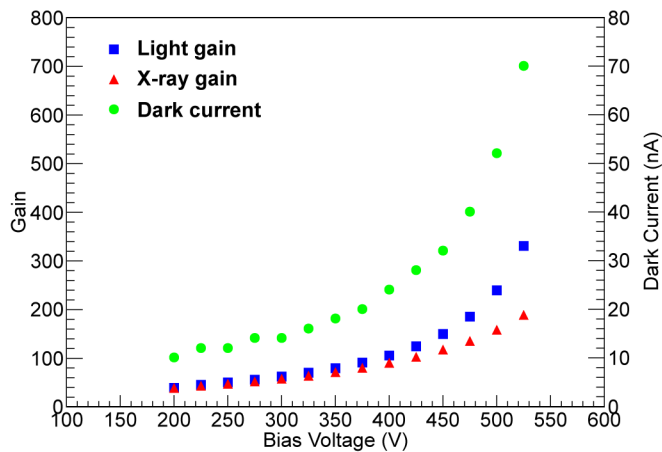


Fig. 3. X-ray and visible light gains as a function of bias voltage for the 5×5 mm² RT-APD at 25 °C. The APD dark current is also plotted.

5×5 mm² RT-APD. The two series of data points were normalized to the manufacturer gain values at 200 V (Table I). In Fig. 3 is also displayed the dark current measured during measurements. As expected, light gain is higher than X-ray gain, increasing significantly for voltages above 400 V. Similarly, the dark current increases with increasing bias voltage, limiting the energy resolution obtained at higher bias voltages, as it will be shown in Section IV.

In Fig. 4 the ratio between 8 keV X-rays and visible light pulses is depicted as a function of the reverse bias voltage for different temperatures. The variation is not very large for lower voltages, increasing significantly for voltages above 300 V. The gain non-linearity increases with decreasing temperature. At 350 V, the gain non-linearity obtained for -20 °C, 0 °C and 20 °C is 25%, 18% and 10%, respectively. These results are in agreement with those obtained in [24], where a non-linearity of 46% was obtained for 5.9 keV X-rays at 415 V. Nevertheless, the achieved values are significantly larger when compared to other types of APDs. For instance, at a gain of 200 and for 5.9 keV X-rays, gain non-linearities between 7% and 10% were measured with LAAPDs from Adanced Photonics Inc. [11]. For 5.4 keV X-rays and at a gain of 400, a 10% deviation was obtained for LAAPDs from Radiation Monitoring Devices [22]. However, as stated in [25], the non-linearities obtained for prototypes with larger active areas are smaller when compared with those with smaller areas, the latter reaching gain non-linearities up to 30% to 50% for 5.9 keV X-rays at a gain of 100.

C. Temperature Dependence

Gain measurements have been performed at different temperatures for X-rays. Normalization to the gain provided by the manufacturer at 200 V and 25 °C has been made. The trend observed at room temperature are reproduced also at lower temperatures: the gain increases with increasing voltage for both RT-APDs and decreases with increasing temperatures, as seen in Fig. 5 for the 5×5 mm² RT-APD type. For 350 V, the gain obtained at -20 °C is about twice the gain obtained at 20 °C.

In Fig. 6, the X-ray gain is plotted as a function of temperature for different bias voltages, for the 5×5 mm² RT-APD. For a given bias voltage, the X-ray gain increases with decreasing

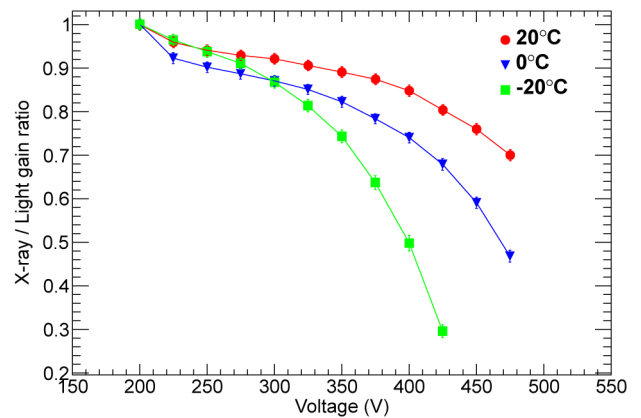


Fig. 4. Gain non-linearity between X-rays and visible light pulses for the 5×5 mm² RT-APD as a function of the light gain for different temperatures.

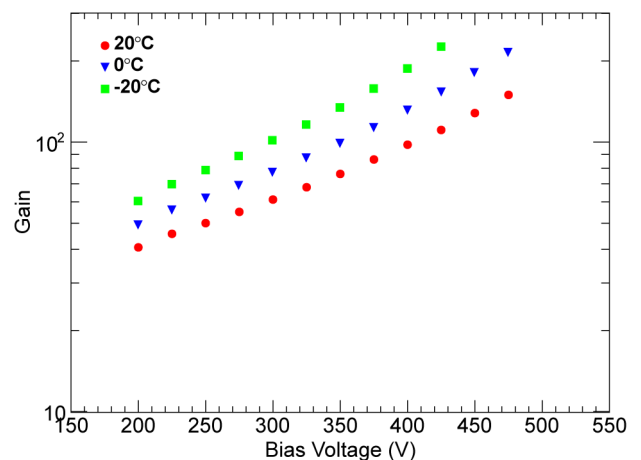


Fig. 5. X-ray gain as a function of bias voltage for different operation temperatures for the 5×5 mm² RT-APD.

temperature, as expected. For each voltage applied, the relative gain variation (in %) is approximately constant in the temperature range between -20 °C and 20 °C, as shown by the exponential fits in Fig. 6. The gain variation with temperature increases with bias voltage, being -1.0% per °C at 200 V and -1.7% per °C at 400 V. Comparable results were obtained for the 3×5 mm² prototype. Nonetheless, the variation is smaller than the one reported for other types of APDs [4], [22], where relative variations of -4.5% per °C were measured for the higher voltages applied. Even for the same type of RT-APDs, our result is smaller, than the one reported in [14], where a variation of -2.2% per °C was found at 200 V.

IV. RESPONSE IN X-RAY DETECTION

The response of the RT-APDs has been evaluated in view of their implementation as X-ray detectors in the muonic helium Lamb shift experiment. The performance characteristics in the detection of 8 keV X-rays have been measured at different temperatures, including energy resolution and minimum detectable energy. Fig. 7 shows a typical energy spectrum for 8 keV X-rays, obtained for both RT-APDs at 0 °C. The distributions are normalized to the same number of events in the X-ray peak region. The X-ray distribution of the 5×5 mm²

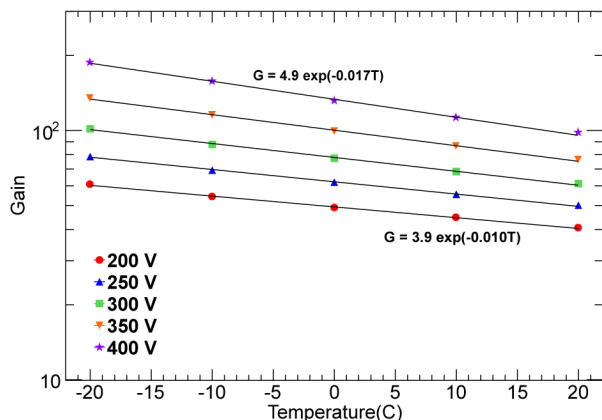


Fig. 6. X-ray gain as a function of temperature for the 5×5 mm² RT-APD prototype at different bias voltages. Exponential fits to data points are shown.

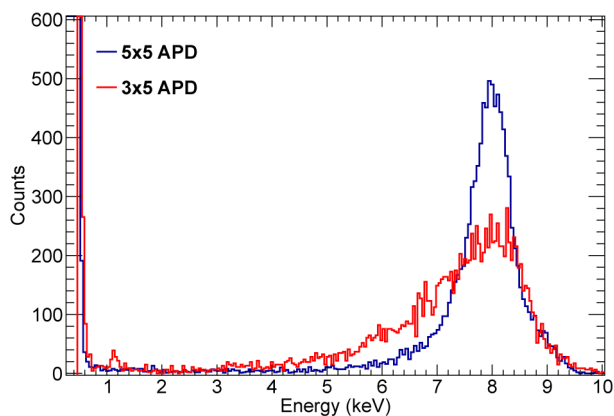


Fig. 7. Typical energy distributions for 8 keV X-rays, obtained with two RT-APDs prototypes at 0 °C for $V = 300$ V.

prototype presents a well-defined Gaussian distribution, while the 3×5 mm² prototype shows larger asymmetry to the left of the X-ray peak, compromising the energy resolution obtained. Therefore, since just one prototype of each size was tested, solid conclusions cannot be driven by the trend shown. More prototypes needed to be tested to understand in full detailed what was the cause beyond this performance.

However, there is no significant tail towards the low-energy region, for both RT-APDs, unlike what has been reported in [11] and [22]. This reveals that almost all the 8 keV X-rays are fully amplified. The electronic noise tail observed in the energy distributions determines the minimum detectable X-ray energy.

A. Energy Resolution

The energy resolution is determined by several factors, such as statistical fluctuations in the number of primary electron-hole pairs and in the number of secondary electrons (gain) produced in the avalanche process, gain variations associated to non-uniform silicon resistivity and noise associated to the detector dark current and to the electronic system [11]. The gain non-uniformity affects the X-ray energy resolution due to the point-like absorption of the X-ray, while in light detection the primary electron-hole pairs are spread over the RT-APD volume [11], [23].

The energy resolution for 8 keV X-rays obtained at 20 °C in both RT-APDs is depicted in Fig. 8 as a function of the X-ray

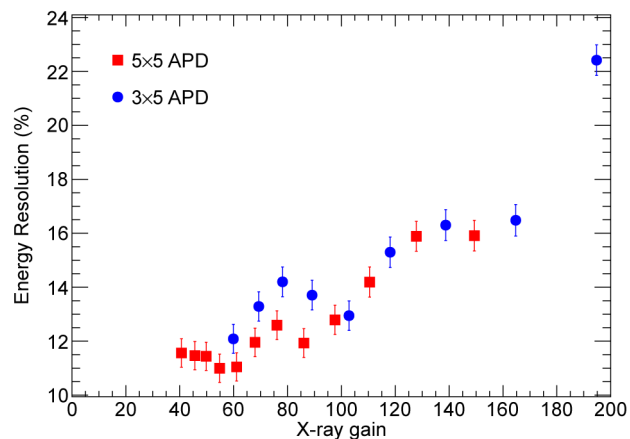


Fig. 8. Energy resolution for 8 keV X-rays as a function of X-ray gain, obtained at 20 °C for both 5×5 mm² and 3×5 mm² prototypes.

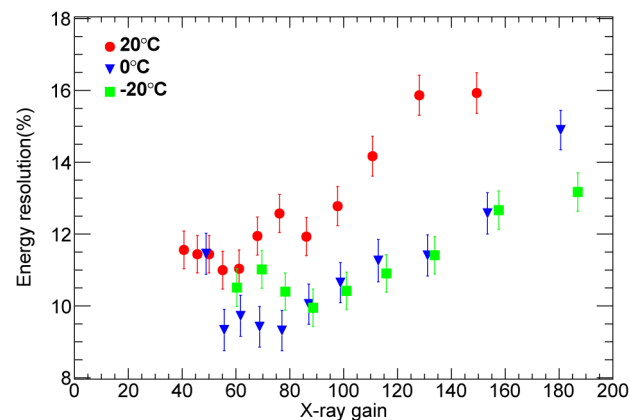


Fig. 9. Energy resolution for 8 keV X-rays as a function of gain, obtained in the 5×5 mm² prototype at different temperatures.

gain. The best energy resolution achieved is 11% (FWHM) for the 5×5 mm² prototype, obtained at a gain of 55. For the 3×5 mm² prototype, the minimum value is 12.1% at a gain of 60. It is observed that the energy resolution degrades for higher gains. This is due to the increase of the dark current (see Fig. 3).

The temperature dependence of the energy resolution is shown in Fig. 9. As expected, and similar to APDs from references [4] and [22], the energy resolution improves for lower temperatures and degrades for higher gains due to the increase in bias voltage resulting in large local differences of the electric field and consequently larger differences in the avalanche multiplication gain. There is no significant improvement in the energy resolution below 0 °C. The best energy resolution of 9.5% was achieved at 0 °C for a gain of 55.

B. Minimum Detectable Energy

The minimum detectable energy (MDE) is defined as the channel in the spectrum where the number of counts in the noise distribution reaches 10% of the counts at the height of the X-ray distribution (centroid channel), the MDE being the corresponding energy at the channel normalized to the centroid of the 8 keV X-ray peak. The MDE as a function of gain for both RT-APDs at 0 °C is presented in Fig. 10. The MDE decreases with gain and is lower for the smaller prototype, although this

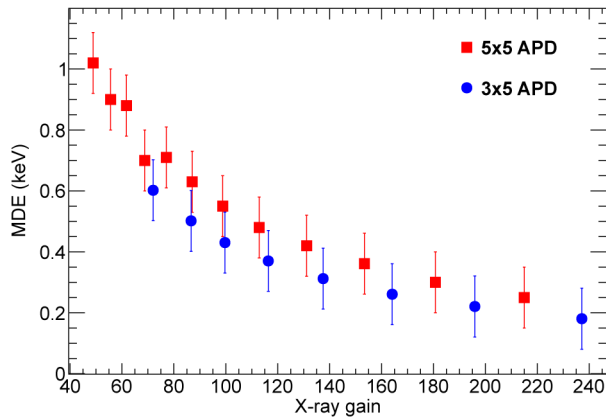


Fig. 10. Minimum detectable energy as a function of X-ray gain for both $5 \times 5 \text{ mm}^2$ and $3 \times 5 \text{ mm}^2$ RT-APDs at $0 \text{ }^\circ\text{C}$.

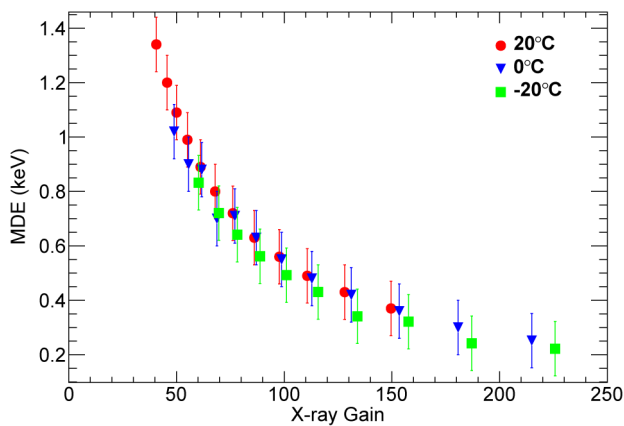


Fig. 11. Minimum detectable energy as a function of X-ray gain for the $5 \times 5 \text{ mm}^2$ prototype at different temperatures.

difference is not significant. The best MDE value obtained is about 0.25 keV for higher gains; however, it is 0.9 keV in the gain region corresponding to the best energy resolution. The MDE was determined for different temperatures, see Fig. 11 for the $5 \times 5 \text{ mm}^2$ RT-APD. MDE has a fast initial decrease with gain and tends to stabilize for high gains. It improves with decreasing temperature. Still this behaviour is not as significant as for other types of APDs [11].

V. CONCLUSIONS

The new muonic helium experiment is being prepared at PSI and requires the use of X-ray detectors for 8 keV X-rays emitted by muonic helium ions. In the preceding muonic hydrogen Lamb shift experiment the detectors chosen for 1.9 keV X-rays emitted by muonic hydrogen atoms were planar LAAPDs from Radiation Monitoring Devices. RT-APDs with a depletion region as thick as $130 \text{ }\mu\text{m}$ were investigated as possible X-ray detectors to be used in the muonic helium experiment. Two prototypes from Hamamatsu Photonic with $5 \times 5 \text{ mm}^2$ and $3 \times 5 \text{ mm}^2$ active areas were investigated. The best performance was achieved by the larger prototype. The best energy resolution achieved is 9.5% at $0 \text{ }^\circ\text{C}$ and the minimum detectable energy attained is 0.25 keV. However, it

is 0.9 keV in the gain region corresponding to the optimum energy resolution. The gain variation with temperature was found to increase with bias voltage, its relative variation being -1.0% per $^\circ\text{C}$ and -1.7% per $^\circ\text{C}$ for 200 V and 400 V, respectively. The gain non-linearity between X-rays and visible light pulses, was also investigated, showing an increase with decreasing temperatures. Indeed, for a bias voltage of 350 V at $-20 \text{ }^\circ\text{C}$ a gain non-linearity of 25% is obtained, whereas at $20 \text{ }^\circ\text{C}$ it is 10%. As a result of these values, the RT-APD prototype investigated have shown much worse performance than the planar APDs used before. In addition larger prototypes would be needed to cover the solid angle around the helium target in the experiment.

ACKNOWLEDGMENT

The authors would like to thank the Paul Scherrer Institute where this work was carried out.

REFERENCES

- [1] D. Renker and E. Lorenz, "Advances in solid state photon detectors," *JINST*, vol. 4, p. P04004, 2009.
- [2] D. Renker, "Properties of avalanche photodiodes for applications in high energy physics, astrophysics and medical imaging," *Nucl. Instrum. Meth. A*, vol. 486, pp. 164–169, 2002.
- [3] F. Mulhauser, L. M. P. Fernandes, A. Antognini, M. Boucher, C. A. N. Conde, and O. Huot *et al.*, "Application of large-area avalanche photodiodes to X-ray spectrometry of muonic atoms," *Spectroc. Acta B*, vol. 58, pp. 2255–2260, 2003.
- [4] L. M. P. Fernandes, J. A. M. Lopes, J. M. F. dos Santos, P. E. Knowles, L. Ludhova, and F. Mulhauser *et al.*, "LAAPD low temperature performance in X-ray and visible-light detection," *IEEE Trans. Nucl. Sci.*, vol. 51, no. 4, pp. 1575–1580, Aug. 2004.
- [5] T. Ikagawa, J. Kataoka, Y. Yatsu, N. Kawai, K. Mori, and T. Kamae *et al.*, "Performance of large-area avalanche photodiode for low-energy X-rays and γ -rays scintillation detection," *Nucl. Instrum. Meth. A*, vol. 515, pp. 671–679, 2003.
- [6] S. Tanaka, J. Kataoka, Y. Kanai, Y. Yatsu, M. Arimoto, and M. Koizumi *et al.*, "Development of wideband X-rays and γ -ray spectrometer using transmission-type, large-area APD," *Nucl. Instrum. Meth. A*, vol. 582, pp. 562–568, 2007.
- [7] R. B. Gomes, C. H. Tan, P. J. Ker, J. P. R. David, and J. S. Ng, "InAs avalanche photodiodes for X-ray detection," *JINST*, vol. 6, p. P12005, 2011.
- [8] T. R. Gentile, M. Bales, U. Arp, B. Dong, and R. Farrel, "Response of large area avalanche photodiodes to low energy x rays," *Rev. Sci. Instrum.*, vol. 83, pp. 053105-1–053105-9, 2012.
- [9] K. Ogasawara, F. Allegrini, M. I. Desai, S. Livi, and D. J. McComas, "A linear mode avalanche photodiode for ion detection in energy range 5–250 keV," *IEEE Trans. Nucl. Sci.*, vol. 59, no. 5, pp. 2601–2607, Oct. 2012.
- [10] S. Kasahara, T. Takashima, and M. Hirahara, "Variability of the minimum detectable energy of an APD as an electron detectors," *Nucl. Instrum. Meth. A*, vol. 664, pp. 282–288, 2012.
- [11] L. M. P. Fernandes, F. D. Amaro, A. Antognini, J. M. R. Cardoso, C. A. N. Conde, and O. Huot *et al.*, "Characterization of large avalanche photodiodes in X-ray and VUV-light detection," *JINST*, vol. 2, p. P08005, 2007.
- [12] M. Moszynski, M. Szawlowski, M. Kapusta, M. Balcerzyk, and D. Wolski, "Large area avalanche photodiodes in scintillation and X-rays detection," *Nucl. Instrum. Meth. A*, vol. 485, pp. 504–521, 2002.
- [13] J. Kataoka, T. Saito, Y. Kuramoto, T. Ikagawa, Y. Yatsu, and J. Kotoku *et al.*, "Recent progress of avalanche photodiodes in high-resolution X-rays and γ -rays detection," *Nucl. Instrum. Meth. A*, vol. 541, pp. 398–404, 2005.
- [14] Y. Yatsu, Y. Kuramoto, J. Kataoka, J. Kotoku, T. Saito, and T. Ikagawa *et al.*, "Study of avalanche photodiodes for soft X-ray detection below 20 keV," *Nucl. Instrum. Meth. A*, vol. 564, pp. 134–143, 2006.
- [15] Hamamatsu Photonics K.K., 1126-1, Ichino-cho, Higashi-ku, Hamamatsu City, Shizuoka Pref., 435-8558, Japan.
- [16] Perkin Elmer, Inc., 940 Winter Street, Waltham, MA 02451 USA.

- [17] A. Antognini, F. Biraben, J. M. R. Cardoso, D. S. Covita, A. Dax, and L. M. P. Fernandes *et al.*, "Illuminating the proton radius conundrum: The mu He + lamb shift," *Canad. J. Phys.*, vol. 89, pp. 47–57, 2011.
- [18] R. Pohl, A. Antognini, F. Nez, F. D. Amaro, F. Biraben, and J. M. R. Cardoso *et al.*, "The size of the proton," *Nature*, vol. 466, pp. 213–216, 2010.
- [19] A. Antognini, F. Nez, K. Schuhmann, F. D. Amaro, F. Biraben, and J. M. R. Cardoso *et al.*, "Proton structure from the measurements of 2S-2P transition frequencies of muonic hydrogen," *Science*, vol. 339, pp. 417–420, 2013.
- [20] RMD, Inc., 44 Hunt Street, Watertown, MA 02472 USA.
- [21] CLRC Rutherford Appleton Laboratory, Chilton, Didcot, Oxfordshire, OX11 0QX, U.K.
- [22] L. Ludhova, F. D. Amaro, A. Antognini, F. Biraben, J. M. R. Cardoso, and C. A. N. Conde *et al.*, "Planar LAAPDs: Temperature dependence, performance, and application in low-energy X-ray spectroscopy," *Nucl. Instrum. Meth. A*, vol. 540, pp. 169–179, 2005.
- [23] L. M. P. Fernandes, J. A. M. Lopes, J. M. F. dos Santos, and C. A. N. Conde, "Application of large-area avalanche photodiodes to energy-dispersive x-ray fluorescence analysis," *X-Ray Spectrom.*, vol. 30, pp. 164–169, 2001.
- [24] T. Lux, E. D. C. Freitas, F. D. Amaro, O. Ballestar, G. V. Jover-Manas, and C. Martín *et al.*, "Characterization of the hamamatsu S8664 avalanche photodiodes for x-ray and VUV-light detection," *Nucl. Instrum. Meth. A*, vol. 685, p. 11, 2012, [arXiv:1108.5143].
- [25] M. Moszynski, M. Kapusta, M. Balcerzyk, M. Szawłowski, and D. Wolski, "Large area avalanche photodiodes in X-ray and scintillation detection," *Nucl. Instrum. Meth. A*, vol. 442, pp. 230–237, 2000.